

Design and Control of a Mechatronic Tracheostomy Tube for Automated Tracheal Suctioning

Thanh Nho Do*, *Member, IEEE*, Tian En Timothy Seah, and Soo Jay Phee, *Member, IEEE*

Abstract—Goal: Mechanical ventilation is required to aid patients with breathing difficulty to breathe more comfortably. A tracheostomy tube inserted through an opening in the patient neck into the trachea is connected to a ventilator for suctioning. Currently, nurses spend millions of person-hours yearly to perform this task. To save significant person-hours, an automated mechatronic tracheostomy system is needed. This system allows for relieving nurses and other carers from the millions of person-hours spent yearly on tracheal suctioning. In addition, it will result in huge healthcare cost savings. **Methods:** We introduce a novel mechatronic tracheostomy system including the development of a long suction catheter, automatic suctioning mechanisms, and relevant control approaches to perform tracheal suctioning automatically. To stop the catheter at a desired position, two approaches are introduced: 1) Based on the known travel length of the catheter tip; 2) Based on a new sensing device integrated at the catheter tip. It is known that backlash nonlinearity between the suction catheter and its conduit as well as in the gear system of the actuator are unavoidable. They cause difficulties to control the exact position of the catheter tip. For the former case, we develop an approximate model of backlash and a direct inverse scheme to enhance the system performances. The scheme does not require any complex inversions of the backlash model and allows easy implementations. For the latter case, a new sensing device integrated into the suction catheter tip is developed and backlash compensation controls are avoided. **Results:** Automated suctioning validations are successfully carried out on the proposed experimental system. Comparisons and discussions are also introduced. **Significance:** The results demonstrate a significant contribution and potential benefits to the mechanical ventilation areas.

Index Terms—Backlash compensation, mechanical ventilation, suction catheter, tracheal suctioning, tracheostomy tube.

I. INTRODUCTION

MECHANICAL ventilation is a process whereby patients are supported with artificial breathing machines, usually in intensive care units (ICUs) [1]. In this process, oxygen is pushed into one's lungs and carbon dioxide is removed. An endotracheal tube is inserted through the mouth into the trachea to facilitate this. There are multiple indications for mechanical

Manuscript received February 7, 2015; revised August 22, 2015 and September 7, 2015; accepted October 13, 2015. Date of publication October 15, 2015; date of current version May 18, 2016. This work was supported by Ministry of Education, Singapore, under the Grant RGT16/13 in collaboration with Intensive Care Unit of Singapore's National University Hospital. *Asterisk indicates corresponding author.*

*T. N. Do is with the School of Mechanical and Aerospace Engineering, Nanyang Technological University, Singapore, 639798 (e-mail: thanh4@e.ntu.edu.sg).

T. E. T. Seah and S. J. Phee are with the School of Mechanical and Aerospace Engineering, Nanyang Technological University.

Color versions of one or more of the figures in this paper are available online at <http://ieeexplore.ieee.org>.

Digital Object Identifier 10.1109/TBME.2015.2491327

ventilation. Up to 20 million patients worldwide are mechanically ventilated each year [2]. Unfortunately, it is not always easy to liberate patients from mechanical ventilation. At least 13% of these patients require prolonged mechanical ventilation [3]. In such patients, it is not feasible and extremely uncomfortable to leave the endotracheal tubes in the patients mouths and trachea [4], [5]. It is estimated that 5–10% of mechanically ventilated patients require a tracheostomy tube and this translates to at least 1 million tracheostomies performed around the world per year [6], [7].

Essentially, a tracheostomy tube is often inserted through an opening in the neck into the trachea, below the vocal cords [8]. Patients with a tracheostomy tube often have large amounts of airway secretions. Nurses perform manually suctioning by inserting size 10 to 12 FG catheters through the tracheostomy tube to just 5–10 cm below the level of the tube. These catheters are no larger than half of the inner diameter of the tracheostomy tube [9]. Prolonged manual suctioning is, however, associated with multiple problems. First, studies have found that nurses generally have poor knowledge of recommended best practices for tracheal suctioning [10]. The significance of this knowledge gap becomes clear when one considers the high turnover rate for performing this task. Second, it is not easy to practice strict infection control with appropriate weaning of gloves and eye protection. Third, manual tracheal suctioning is associated with huge healthcare costs [9], [11].

Several studies on the mechanical ventilation system have been proposed in the literature. Most of cases focus on the localization methods to determine the position between the endotracheal tube and the carina. For example, Shamir *et al.* [12] introduced a new concept for endotracheal tube positioning using visual images. Lederman *et al.* [13], [14] designed a novel visual system for endotracheal tube position confirmation based on video image classifications. Song *et al.* [15] used an infrared sensor stylet to position an endotracheal tube at the correct depth. Kato *et al.* [16] used a Visual Stethoscope to accurately locate the tracheal tube on the bronchial side of the carina. Goethals *et al.* [17] introduced a novel airway device with tactile sensor to determine the endotracheal tube position. Moll *et al.* [18] compared the three different approaches for positioning of the tracheal tube tip. It was concluded that the main stem intubation technique gave the best positioning results compared to the depth and the cuff palpation techniques. Although these aforementioned methods offer goods results for positioning the endotracheal tube, no complete mechatronic systems for automated tracheal suctioning are introduced so far.

Motivate from these aforementioned approaches and to do away with multiple problems associated with manual tracheal

suctioning, we propose a novel design for a mechatronic tracheostomy system that incorporates a translation gear system, a new robotic catheter, an electronic suction pump, a tracheostomy tube, a new sensing device, and a real-time controller for automated tracheal suctioning. A critical search reveals that hospitals all over the world are using the conventional manual method of clearing mucus. We aim to automate this process mainly to reduce manpower required for suctioning and to increase the independence of such patients so that more health-care costs could be reduced. In addition, the proposed suction catheter is designed to have a longer length (around 2 m) compared to a commercial catheter available in the market (0.4 m). To stop the catheter at a desired position for suctioning, two control approaches are presented and discussed: 1) based on the known travel length of catheter tip; 2) Based on a new sensing device integrated at the catheter tip.

For the former, a new compensation control scheme will be introduced to improve the tracking performances of the designed system. It is known that the nonlinear friction and backlash are inherent in the gear system, linear guide, and the suction catheter. These factors cause poor performances for the system. Various studies on backlash, hysteresis models, and compensation control have been proposed and discussed in the literature [19]–[26]. For example, Kesner and Howe [20] implemented a backlash width-based compensation method to improve the tracking performances without considering the backlash slopes. Bardou *et al.* [23] compensated the backlash hysteresis in a flexible endoscope using a look-up table to estimate the dead band. Although these studies are able to characterize the friction and backlash in the robotic catheter, tendon-sheath mechanism, endoscope, and gear systems, some limitations still exist. First, they only consider the control problem under the assumptions such as available information of sheath/catheter configuration and continuous measurements of the output position. Second, their compensation schemes require a complex inverse model for the backlash and a discontinuous switching function of velocity. In practice, these works are complex and not easy to implement.

There exist two approaches for the modeling of backlash and hysteresis nonlinearities: discrete models (Presisach, Prandtl–Ishlinskii) and continuous models (Bouc–Wen, Duhem, Dahl) [27]–[32]. These models have several shortcomings for both modeling and control purposes. For example, the Prandtl–Ishlinskii and Preisach are modeled by the sum of many elementary hysteresis namely hysterons, which increase the complexity in implementation and computation if a high number of elements is considered. The Bouc–Wen model needs six parameters in its structure to capture the hysteresis behavior. More time is needed to identify its model parameters. Unlike these aforementioned models, the Dahl model can capture a wide range of hysteresis and possesses simplicity with only three model parameters in its structure [33]. To overcome these aforementioned drawbacks, a new backlash-like hysteresis model and a new direct inverse approach-based feedforward compensation will be developed in this paper. The proposed model is an extended version of the Dahl model that allows to capture a wide range of backlash-like hysteresis phenomena in mechanical systems. Compare to

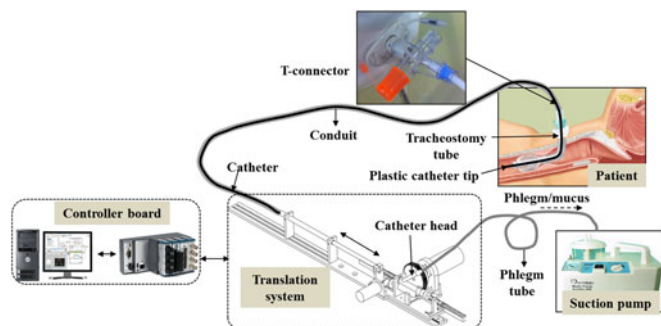


Fig. 1. Illustration of the proposed automated mechatronic tracheostomy tube.

other approaches in the literature, our approach is simple to use for identification and the design of a direct inverse model-based feedforward compensator. The direct inverse compensator does not require any complex inversions of backlash hysteresis model and allows for easy implementations and calculation [28], [34]–[37].

For the latter, a new sensing device will be developed and integrated into the catheter tip. In this case, compensation control schemes for the backlash nonlinearity are avoided. Compare to other approaches on the positioning endotracheal tube [12]–[18], the proposed sensing device is simple and easy to implement. The main function of this sensing device is based on an “ON–OFF” electric circuit. When the catheter is in free motion and/or small compression force applied to the sensing device, there always exists an opened circuit (OFF). However, when this device is in contact with object (dead end) at a compression force level, its inner mechanisms will form a closed electrical circuit (ON). The “ON–OFF” states of this electric circuit control the “STOP–MOVE” of the catheter translation and “OPEN–CLOSE” of the suction pump, respectively.

To demonstrate the effectiveness of the proposed approaches, a new prototype for the mechatronic tracheostomy tube system is developed. Experimental validations are also presented and discussed. The rests of this paper are organized as follow: Section II presents the prototype design for a novel mechatronic tracheostomy tube and the proposed suction catheter. Section III gives compensation control design for the first proposed approach when the travel length of the catheter is known in advance. The sensing device integrated at the catheter tip is introduced in this section. Real-time experimental validations are given in Section IV. Finally, discussion and conclusion are drawn in Section V.

II. SYSTEM DESIGN OF THE AUTOMATED MECHATRONIC TRACHEOSTOMY TUBE FOR TRACHEAL SUCTIONING

A. Overview of the Tracheal Suction Procedure

The concept for a new prototype of the proposed mechatronic tracheostomy tube is depicted in Fig. 1. The designed system consists of a long suction catheter, a storage conduit, a T-connector, a tracheostomy tube, a translation mechanism, an electronic suction pump, and a real-time controller. To enable the motion of the catheter, a translation mechanism is used. One

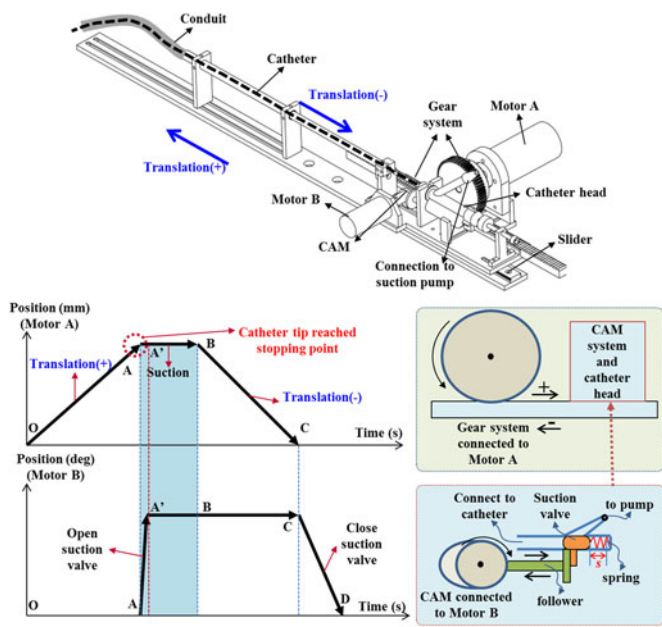


Fig. 2. Translation mechanism and operation principle of the suction system.

end of the storage conduit is connected to the tracheostomy tube via a T-connector, while the other end is connected to a translation mechanism (see Fig. 2). A smaller, thin catheter will be inserted directly into the conduit at regular, timed intervals, and will carry out the suction tasks via the tracheostomy tube. Once completed, the catheter will be pulled back and await the next cycle of the suction (see Fig. 2). The catheter head is connected to a suction pump via a suction valve. This suction valve is controlled by a CAM system via a follower (see Fig. 2). There are two approaches to determine the stopping point for the catheter tip: 1) base on the travel length for the catheter tip. In this case, a first insertion could be done manually by a nurse to measure this travel length; (ii) base on the sensing device integrated at the catheter tip. In this case, no measurements for the travel length of the catheter are required. After the catheter tip has reached the desired stopping point (point A—Fig. 2), the suction valve is automatically opened by the CAM mechanism and a negative pressure from the suction pump will be provided (point A to A'—Fig. 2). Suction, which is turned ON throughout, would cause the mucus accumulated to be sucked out of the patient's body. After a predetermined time interval for suctioning (point A' to B—Fig. 2), the catheter would be pulled out of the patient's body (point B to C—Fig. 2). Finally, the suction valve is closed (point C to D—Fig. 2) and wait for next suction. To prevent the mucus falling back to the carina area and to keep a clear secretion from inside catheter, the suction valve should be continuously opened until the catheter tip is completely removed out of the human body.

There are some clinical requirements/technical specifications for the proposed suction system.

- 1) *Speed of the Insertion:* The speed of catheter insertion can be observed from standard practice among nurses. As recommended from medical doctors at National Univer-

sity Hospital, Singapore, a speed of around 10 mm/s is suitable for use in clinical applications.

- 2) *Tracheostomy Tube and Suction Catheter Size:* A maximum size is recommended because it allows lower resistance to air flow. However, the maximum sizes of the tracheal tube are constrained by the tracheostomy hole. For adults, a tracheal tube inner diameter of 7.5–9.5 mm is recommended. The suction catheter size is closely related. There has to be enough space between the catheter and the tube to allow air inflow from the ventilator. The suction catheter should have an external diameter less than half that of the endotracheal tube inner diameter. For a tracheal tube of 8-mm diameter, this translates to a maximum catheter size of 4-mm outer diameter [38].
- 3) *Suction Pressure Level:* The suction pressure settings are measured when the tip is occluded. Too much suction pressure could result in tissue damage and atelectasis. Too little suction pressure would result in insufficient mass flow especially when the mucus is highly viscous. The general recommendation is to use 80–120 mmHg for adults and 80–100 mmHg for children [39].
- 4) *Duration of Suctioning and Insertion Depth:* Once the bulk of the mucus has been extracted, further suctioning will reduce the lung volume and increase the risk of hypoxia. A suction duration of around 10–15 s for adults and 5 s for pediatrics is recommended for safety. Based on clinical experience and study, it is recommended that the insertion depth should be around 5–10 cm below the level of the tube [40].
- 5) *Sterilization:* The suction catheters are sterilizable in sterile water or a dilute vinegar solution, and can be reused up to a period of 24 h from first usage [41].

B. Suctioning System Design

This section presents the design of a novel mechatronic tracheostomy tube for automated tracheal suctioning.

1) *Translation Mechanism and Suction Valve:* The operation principle and its translation mechanism for the suction system are shown in Fig. 2. The catheter motion is driven by a Faulhaber dc Motor A using a gear system including a spur gear GEAB and a rack gear RGEAS from MITSUMI Electric Company, Ltd. The gear system is fixed on the sliding part of a miniature linear guide SSEBWV from MITSUMI. To control the suction valve located at the catheter head, a CAM mechanism connected to a Faulhaber dc Motor B is used. The catheter head is a Y-shape type where the suction valve can slide within a range of $s = 5$ mm to connect and disconnect the pressure from the pump. In the forward direction, the valve is driven by the CAM mechanism, while in the backward direction, it is driven by a linear spring. All signals in the system are decoded using real-time controller NI cRIO-9076 and NI LabVIEW software from National Instruments, Ltd.

2) *Suction Catheter and its Conduit:* To automate the tracheal suctioning and to adapt with the proposed suction system, the suction catheter must be long and disposable. Current suction catheters available in the market are often short and

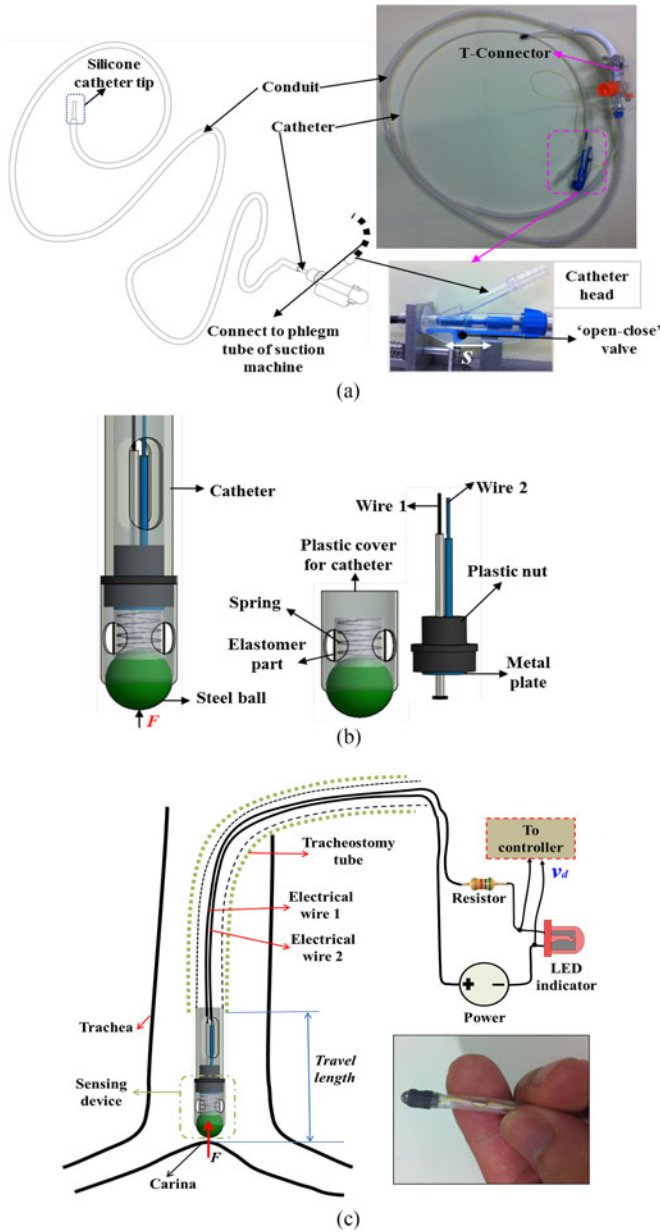


Fig. 3. Suction catheter design. (a) Suction catheter and its conduit with no sensing device. (b) Design for the sensing device at the catheter tip. (c) Suction catheter with sensing device inserted to a tracheostomy tube.

difficult to use in the designed automated suction machine. To deal with these challenges, a new prototype of the flexible suction catheter and its conduit is developed [see Fig. 3(a)]. Both flexible catheter and its conduit are made from Nephron polytetrafluoroethylene material where the catheter tip is made of either flexible silicone or thermosensitive Polyvinylchloride (they are compatible with medical use and disposable as well as identical to current suction catheters in the market) with a length of 400 mm. The catheter possess an inner diameter, outer diameter, and length of 3.5, 4, and 2000 mm, respectively. The 4-mm diameter of the catheter is suitable for use in most patients [38]. The conduit has an inner diameter, outer diameter, and length of 6, 6.5 and 1500 mm, respectively. The design of catheter head

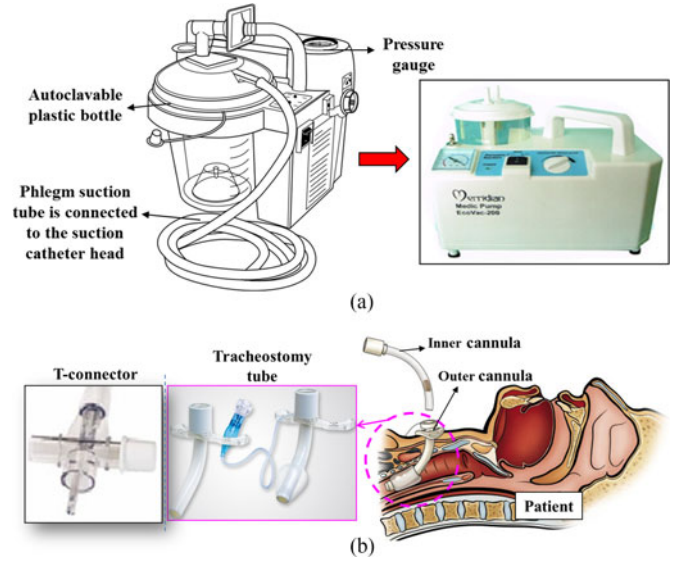


Fig. 4. Off-the-shelf medical equipment for the proposed automated suction system. (a) Portable suction machine. (b) T-connector and tracheostomy tube.

has been given in Section II-A. There are two approaches for the suction catheter design and control

- 1) *Known Travel Length of the Suction Catheter*: In this case, no sensing devices are required at the catheter tip. To determine the travel length for the catheter tip, the first insertion could be done manually by a nurse and this length is utilized for future suction tasks. It was known that backlash and friction that degrade the system performances are unavoidable between the suction and the catheter as well as in the gear system. Hence, compensation control for the backlash is needed to enhance the tracking performances for the system. Detailed developments for this approach will be given in next sections.
- 2) *Unknown Travel Length of the Suction Catheter*: In this case, a sensing device is developed and mounted at the catheter tip as shown in Fig. 3(b) and (c).

3) *Portable Suction Pump, Tracheostomy Tube, and T-Connector*: In this paper, the portable suction pump, tracheostomy tube, and T-connector are off-the-shelf medical equipment. The suction pump that is a type of MERRIDIAN EcoVac-200 7E-A from SANBORN Technologies with a low rate of 18 L/min is used. It is capable of providing up to 560 mmHg of occluded suction pressure [see Fig. 4(a)]. The operated pressure for the suction machine is recommended no higher than 150 mmHg. The tracheostomy tube is attached to a standard sized T-connector, which in turn accepts connections from both the conduit and a ventilation source. Because the used catheter has a size of 4 mm, the required inner diameter of the tracheostomy tube cannula is recommended at least 7.5 mm to allow sufficient space for air from the ventilator to flow. The T-airway connector connected to the inner cannula head is a type of Portex SuctionPro 72 from Smiths Medical with the outlet diameter of 15 mm. The inlet diameter of the T-connector connected to the conduit has a size of 6.5 mm. The rest part

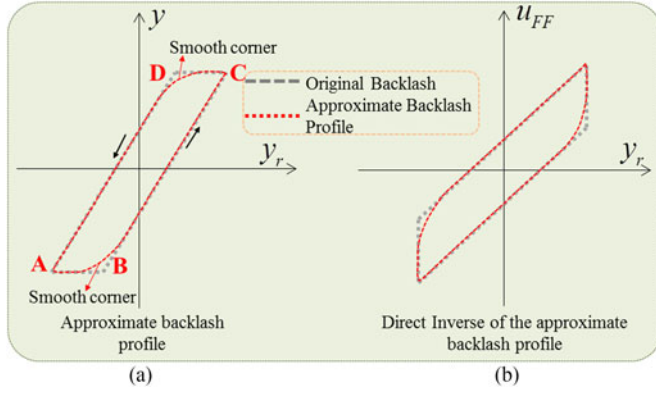


Fig. 5. Approximate backlash profile and its inverse. y_r , y , u_{FF} are desired trajectory, output position, and controller input, respectively.

of the T-connector allows oxygen to go through simultaneously [see Fig. 4(b)].

III. DESIGN FOR COMPENSATION CONTROL AND NEW SENSING DEVICE

To enhance the tracking performances for the system where travel length is known in advance, a backlash-like hysteresis model and its direct inverse that is simple to implement for the identification and control purpose are introduced. In this paper, the proposed model accounts for the backlash between the catheter and its conduit and in the gear system. Fig. 5 illustrates the idea of an approximate model of backlash and its smooth inverse. In the original backlash profile, there is a deadzone (points A-B, C-D), which causes a discontinuity when the system reverses its motion from positive to negative velocity and vice versa [34], [42], [43]. However, this discontinuity can be completely eliminated using an approximate profile of backlash where the corners of original backlash profiles are smoothed out (at points B, D). With this idea, a direct inverse model of the proposed approximate backlash can be used for the controller design. The controller input U_{FF} can be directly extracted from the proposed approximate backlash hysteresis model without using any additional inverse models. The proposed direct inverse method will be given in next sections.

A. New Backlash-Like Hysteresis Model

In this paper, a modified version of the Dahl model that is able to provide an approximate form of the backlash profile in the catheter and gear systems will be used. This model can capture a wide range of hysteresis profile and possesses simplicity with only three model parameters in its structure. It utilizes an internal state, z , and a differential equation to describe the nonlinear backlash-like hysteresis. A simple form of the Dahl model is represented as

$$\dot{z} = \dot{x} - \sigma_0 |\dot{x}| z / F_c \quad (1)$$

$$F = \sigma_0 z \quad (2)$$

where x is the input displacement, F_c is a Coulomb friction force, σ_0 is bristle stiffness, z is internal state that can be obtained from the solution of (1), and F is the output.

In this paper, we are going to enhance the position tracking performances for the system and the force tracking will not be considered. To characterize an approximate form of the backlash profile in the proposed system and to apply the direct inverse model-based feedforward compensation [34], the input displacement x will be considered as the position control input $u_{FF} = x$. Please note that in this attempt, we are going to capture the backlash-like hysteresis profile for the displacement variables (not force variables) at both ends of system, i.e., catheter tip and catheter head positions as illustrated in Fig. 1, to enhance the position tracking performances. Therefore, the displacement x given in (1) will be considered as the input displacement and the variable F in (2) will be considered as the output displacement.

To apply the direct inverse model and to capture the backlash-like hysteresis profile of the displacement, two major modifications will be carried out on the Dahl model. The first modification will replace the velocity \dot{x} in the first term on the right side of (1) by a new scalable term of velocity \dot{x} with a scale factor β . Therefore, (1) can be rewritten as

$$\dot{z} = -\beta \dot{x} - \sigma_0 |\dot{x}| z / F_c = -\beta \dot{x} - \alpha_0 |\dot{x}| z \quad (3)$$

where $\alpha_0 = \sigma_0 / F_c$.

The second modification concerns the extension of (2) to include a new term of displacement with a scale factor $c\sigma_0$ and an offset point y_0 . Then, (2) is rewritten as

$$F = \sigma_0 z + c\sigma_0 x + \sigma_0 y_0 \text{ Or } y = F / \sigma_0 = cx + z + y_0 \quad (4)$$

where x and y denote the input and new output displacements, respectively. $c > 0$ is the backlash-like hysteresis slope. Coefficients $\beta > 0$, $\alpha_0 > 0$. y_0 is an offset point of the displacement y .

The result of (4) represents a straight line of slope c and a smooth hysteresis function z . The new term cx given in (4) is utilized for the design of new controller using a direct inverse from the proposed model. This additional term avoids using the complex inversion in the feedforward compensation of the backlash hysteresis in the system. The direct inverse model-based feedforward compensation scheme will be introduced in next sections.

B. Comparison With the Hysteresis Bouc–Wen Model

The hysteresis Bouc–Wen model has been used in many mechanical applications and it is expressed as [44]

$$\Theta = \alpha_x x + \alpha_\zeta \zeta + \Theta_0 \quad (5)$$

$$\dot{\zeta} = A\dot{x} - B|\dot{x}|\zeta^{m-1} - D\dot{x}|\zeta|^m \quad (6)$$

where Θ and x are the output and input displacement, respectively. α_x and α_ζ are scale factors that represent the ratio of output hysteresis to the input displacement and internal state ζ , respectively. Θ_0 is an offset point with respect to the output displacement. A , B , D , and m are coefficients that control the

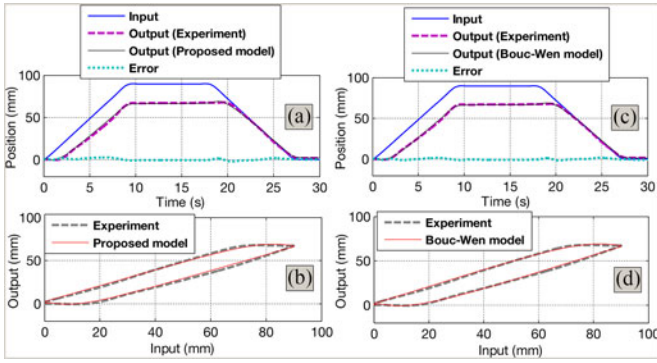


Fig. 6. Identification results. (a) Time history for the identified results using the proposed model. (b) Comparison between the experiment and the proposed model. (c) Time history for the identified results using the Bouc–Wen model. (d) Comparison between the experiment and the Bouc–Wen model.

shape and size of the hysteresis loops. The dot at the top of variables represents the first derivative with respect to time.

The Bouc–Wen model requires six model parameters that sometimes are too cumbersome to identify and to implement in control approach. Fig. 6(c) and (d) shows the capabilities of the Bouc–Wen model given in (5) and (6) to capture the backlash nonlinearity in the system. The experimental data are obtained from Section IV-A.

The optimized parameters for the Bouc–Wen model are first identified using genetic algorithm (GA). GA is a global searching method based on the natural selection and genetics including operators of mutation, crossover, and reproduction [45]–[48]. The GA will generate an initial guess of model parameters. Subsequently, these parameters are refined using Nelder–Mead Simplex method. During the identification process, MATLAB identification toolbox from MathWorks is used. Note that the initial values for the variable z, ζ in (3) and (6) are set to zero. These initial values do not affect the identification results because the GA allows a random selection of initial values for the identification process. The final identified results from GA are refined using the Nelder–Mead Simplex method. The obtained parameters are $A = 1.925, B = 0.091, m = 1.009, D = 1.663, \alpha_x = 0.925, \alpha_\zeta = -0.4533, \Theta_0 = -7.097$. This identification method is also used for the proposed model given by (3) and (4), where the optimized parameters are $\beta = 0.854, \alpha_0 = 0.077, c = 0.9677$, and $y_0 = -7.151$. The root mean squared error (RMSE) for the Bouc–Wen model is 0.8009 mm, while that error for the proposed model is 0.8301 mm. It can be seen that there is a slight difference for the identification error but the proposed approximate model offers less number of model parameters (four parameters). This advantage provides easy identification and implementation. Detailed comparison results are shown in Fig. 6.

C. Direct Inverse Model-Based Feedforward Compensation

In this section, a model-based feedforward compensation control is introduced. Unlike current approaches in the literature that require a smooth backlash inverse and discontinuous switching function of velocity, the proposed control approach in this paper

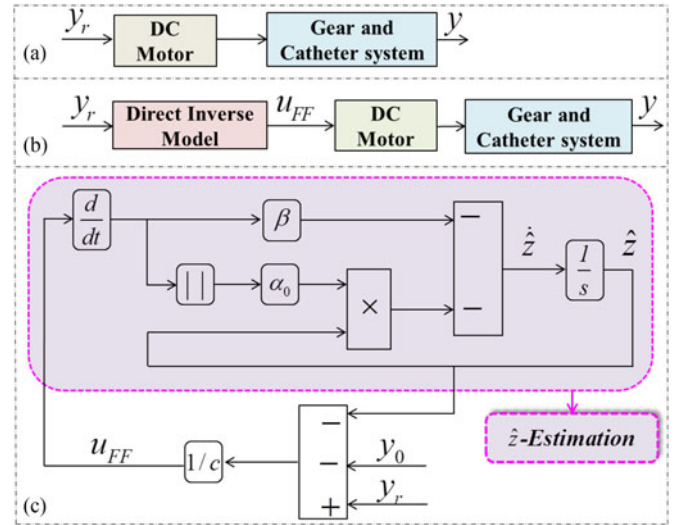


Fig. 7. Control architectures. (a) No compensation scheme. (b) Proposed compensation scheme. and (c) Compensation diagram and estimate of \hat{z} .

uses a form of direct inverse from the model given by (3) and (4) and it is smooth. In current approaches in the literature, the computation of the compensator is an additional work because its parameters have to be likewise computed. In this paper, this addition is avoided. As mentioned in the previous section, the input signal x in (4) will be used as a control input, $x = u_{FF}$. Prescribing a reference signal of displacement, y_r , will result in a new control input u_{FF} generated by the proposed model. Subsequently, a feedforward compensator based on the estimated backlash-like hysteresis \hat{z} and scale factor, c , is given as follows:

$$u_{FF} = (y_r - \hat{z} - y_0)/c. \quad (7)$$

The estimate \hat{z} can be defined as

$$\dot{\hat{z}} = -\beta \dot{u}_{FF} - \alpha_0 |u_{FF}| \hat{z}. \quad (8)$$

By substituting (7) into (4), the relationship between the output displacement, y , and the reference displacement, y_r , is given by

$$y = c(y_r - \hat{z} - y_0)/c + z + y_0 = y_r + (z - \hat{z}). \quad (9)$$

If the value \hat{z} can be accurately predicted, i.e., $\hat{z} = z$, then from (9), the error e_r between the reference trajectory y_r and displacement at the distal end y can be eliminated. It means that y accurately follows the reference signal, y_r . It is also observed that the accuracy of the control scheme depends on the performance of the hysteresis observer given by (8). Note that the variable z is unmeasurable and its estimation \hat{z} is determined based on the estimation structure given in Fig. 7. To implement the proposed approach in the system, a first identification must be carried out to provide a good estimation of the model parameters (β, α_0, c, y_0). Using the identified results and the desired trajectory y_r as the input to the block diagram, the controller U_{FF} can be obtained as shown in Fig. 7(c). The whole process for obtaining U_{FF} is named direct inverse approach and they are carried out using MATLAB Simulink toolbox from MathWorks. It can be seen that the compensator does not require any inversion except for the positive parameter c . In addition,

no additional computation works are required since the model parameters have been known during the modeling and identification process.

D. New Sensing Device

The operation principle of the device is based on a switching circuit. An opened circuit always exists if the compression force F (catheter tip touches a dead end) applied to the device does not exceed a force level F_{\max} . The proposed circuit is connected to an LED indicator (for easy observation), a resistor, and dc power supply [see Fig. 3(c)]. Once this force reaches F_{\max} , a closed circuit is formed and the LED indicator is ON. Then, an electric signal $v_d = 2$ V from a dc power supply is sent to the controller and the motor A is stopped (at point A—Fig. 2). At the same time, the motor B starts to move and opens the suction valve (points A to A'—Fig. 2). The sensing device consists of a steel ball, a linear spring, electrical wires 1, 2, an elastomer part, a plastic nut, a metal part connected to the electrical wire 2, and a plastic cover for the catheter head. The linear spring is connected to both the steel ball and the metal plate. The elastomer part is a cylinder-type with a wall thickness around 0.1 mm. This elastomer that is made from SYLGARD 184 SILICONE ELASTOMER KIT is used to prevent the phlegm leakage from outside. 3-D printer Fortus 250 mc from Stratasys, Ltd. is used to create the mold for the elastomer part. The two electrical wires with outer diameters of 0.2 mm are routed along the catheter. One end is connected to a metal plate fixed on the plastic nut, while the other end is placed inside the spring. When the catheter tip touches the dead end, the steel ball that is pushed to a force F_{\max} will slide toward the spring side and contacts with the wire 2. As a result, a closed circuit is formed.

IV. REAL-TIME EXPERIMENTAL VALIDATIONS

To demonstrate the effectiveness of the proposed control scheme and the proposed sensing device, real-time experiments for the suction system are carried out in this section.

A. Experimental Setup

The photo of experimental setup is shown in Fig. 8. The system consists of a translation system, a catheter and its conduit, an electric suction pump, a tracheostomy tube, a rubber trachea, a displacement laser sensor, and controller board. The PD controller is used to control the motors with gains $P = 10$, $D = 10$. The PD parameters are online tuned based on the trial and error methods. The motor A is connected to a gear system including a spur gear and a rack gear. For the first case where the travel length of the catheter is known in advance, the suction catheter is required to move with a predetermined travel length and a velocity of around 1cm/s (see Section II-A) and return to its starting position with the same velocity after carrying out the suction task. For the second case where the travel length is unknown, the sensing device that is introduced in previous sections will be used to stop the catheter once it reaches the carina (dead point). For both cases when the catheter has reached the desired position, the motor A is stopped at this position around five to

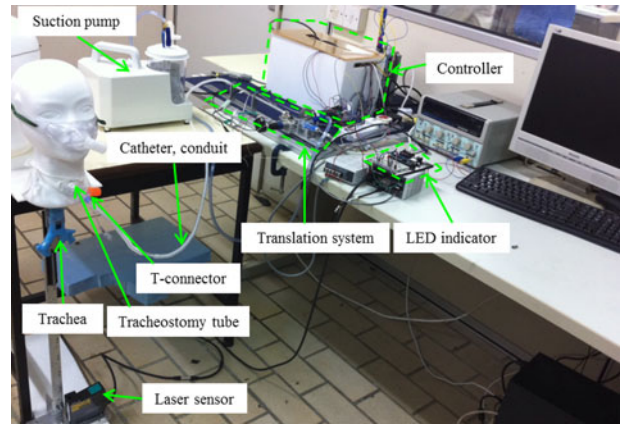


Fig. 8. Photo of the experimental setup.

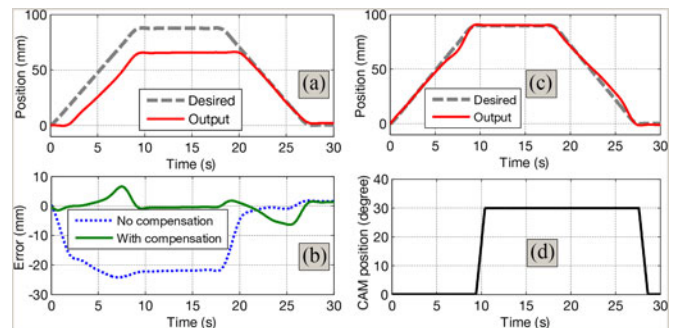


Fig. 9. Compensation result with known travel length of 90 mm and suction time of 9 s. (a) Time history of tracking position with no control scheme. (b) Time history of tracking position with proposed control scheme. (c) Tracking error. (d) Trajectory of motor B-CAM for suction.

ten seconds for suctioning. At the same time, the motor B that is driven by a PD controller ($P = 7$, $D = 7$) and connected to the CAM mechanism starts to rotate (around 30° , rate of $15^\circ/\text{s}$) to open the suction valve. For better illustration, a rubber trachea that possesses a similar size of human trachea is also used in the experimental process [49]. To record the catheter tip displacement, a laser sensor LK-G402 from KEYENCE Singapore Pte, Ltd., is used.

B. Validation for the Proposed Compensation Scheme

For the first case, the objective is to control the catheter tip position y to accurately follow a given desired trajectory y_r with a known travel length. Five trials will be carried out. For illustration, one of five trials is presented only. For easy observation and comparison, Fig. 7(b) and (a) introduces the control structures with and without using the compensation scheme, respectively. Fig. 9 shows the validation results for the proposed control scheme. The catheter tip is controlled to reach a known travel length of 90 mm (distance from the lower part of the tracheostomy tube to the carina) with a given rate of 9 mm/s. These values were recommended by medical doctors from National University of Hospital, Singapore. The model parameters for the suction compensation control that are used

TABLE I
QUANTITATIVE MEASURES RMSE USING THE DESIGNED CONTROLLER

Trials	Before Compensation (mm)	After Compensation (mm)
1	15.413	2.4578
2	15.552	2.2243
3	16.011	2.5527
4	14.998	2.3692
5	16.189	2.6032

for the control purpose were identified in previous sections. It can be observed that the position of catheter tip always lags behind the desired trajectory if no compensation control scheme is used see Figs. 7(a) and 9(a)]. However, the catheter tip position is able to accurately track the desired trajectory when the proposed compensation scheme is applied see Figs. 7(b) and 9(b)]. There is a decrease of the tracking error $e_r = y - y_r$ (e.g., before compensation: RMSE = 15.413 mm; after compensation: RMSE = 2.4578 mm). Once the tip has reached 90 mm in the forward direction, the suction valve is opened by the CAM mechanism connected to the motor B [see Fig. 9(d)]. The catheter is pulled back to its initial position after a suction time of 9 s is carried out. Then, the suction valve is closed and awaits for next suction. Detailed validation results for the trials are shown Table I.

C. Validation for the Proposed Sensing Device

Real-time experiments are carried out on the proposed sensing device using a speed of 9 mm/s for the catheter motion. A virtual rubber trachea that follows the recommended dimension of the normal human trachea and anatomical structure is also used [49]. It is noted that the travel length information for the motor A is not required in advance. The motor A is freely rotated to move the suction catheter toward the carina area. Different travel distances ($L = 65$ mm, $L = 55$ mm, $L = 45$ mm) are applied for the validation purposes. For each experiment, the catheter tip that is routed inside the tracheostomy tube is located at a distance L from the carina point. The motor A is expected to stop the catheter tip once it touches the carina (at a distance L from its initial position). The laser sensor is used to monitor the travel length during the experiments. When the catheter tip touches the carina point, a closed circuit is formed and an electric signal v_d will be sent to the controller. Then, the motor A is stopped. Simultaneously, the motor B starts to rotate and the suction valve is opened. The validation is based on the completion of suction tasks and the achievement of the desired value L for the suction catheter tip. The average force measurement for the proposed sensing device is shown in Fig. 10. Five measurements are carried out using the force sensor LSB200 from FUTEK. To close the electric circuit and to generate the signal v_d , a small force of $F = 0.08017$ N is needed. The validation results for three different values of L are shown in Fig. 11. It can be seen that the sensing device is able to stop the Motor A connected to the catheter and start the Motor B when its tip touches the carina area. All suction tasks are successfully carried out. The five trials are carried out for each value of L . It can be seen

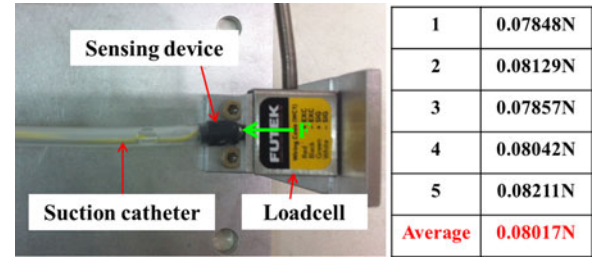


Fig. 10. Force measurement for the sensing device touched a dead end.

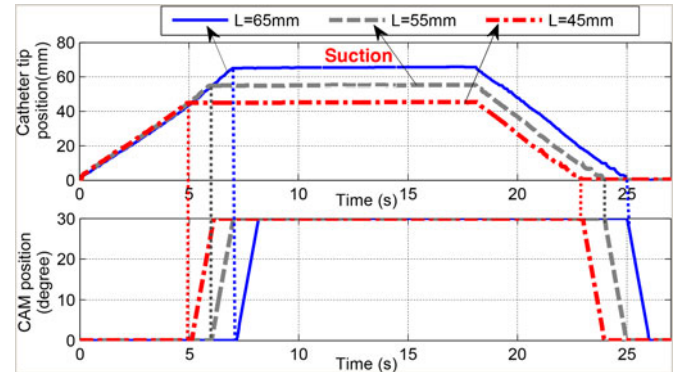


Fig. 11. Validation result for the sensing device with different distances L from the carina. (Upper) Time history of catheter tip position using the sensing device. (Lower) Time history of the CAM connected to Motor B.

TABLE II
QUANTITATIVE MEASURES FOR THE PROPOSED SENSING DEVICE

Trials	$L = 65$ mm	$L = 55$ mm	$L = 45$ mm
1	65.217 mm	54.578 mm	45.716 mm
2	65.432 mm	55.293 mm	46.027 mm
3	64.782 mm	55.187 mm	45.008 mm
4	66.008 mm	56.337 mm	45.192 mm
5	65.599 mm	54.918 mm	44.988 mm
Mean	65.4076 mm	55.2626 mm	45.3862 mm

that the catheter is stopped once the sensing device is triggered. There is a small error between the desired travel length and the measured length (0.4076 mm, 0.2626 mm, and 0.3862 mm for $L = 65$ mm, $L = 55$ mm, and $L = 45$ mm, respectively). The reason is that the catheter tip is forced by a dead end (carina) and this results in little buckle for the catheter. However, these errors are not significant and acceptable. Detailed comparisons are shown in Table II.

V. DISCUSSION AND CONCLUSION

In this paper, we have introduced the development, compensation control, and design for sensing device of a novel mechatronic tracheostomy tube for automated tracheal suctioning. To enhance the performances of the system where the travel length of the suction catheter is known in advance, a modified version of the Dahl model is developed and explored for use with a

feedforward compensator. The proposed model is an approximate form of backlash and it is able to provide a smooth profile of the backlash namely backlash-like hysteresis in the gear system and the robotic catheter. Compare to other model approaches in the literature like Bouc–Wen model, the proposed model is simpler for identification and implementation. The feedforward control scheme does not require the reevaluation of the parameters of the inverse model. The main advantages of this proposed structure are the simplicity of computation and implementation. No model inversions are required since the compensator is always available if the direct model is identified. As a result, no additional computation work is required. The proposed control approaches have been successfully validated on the designed automated mechatronic tracheostomy system and suction tasks have been successfully carried out on a rubber human trachea. This is the first time a direct inverse model-based feedforward is applied to an automated mechatronic tracheostomy system.

A sensing device is used to determine the stopping point for the catheter when the travel length of the catheter is unknown in advance. In this case, the use compensation control schemes is avoided. Compare to other approaches in the literature, the developed sensing device is simple and easy to implement. With a small size of around 4 mm for the suction catheter, it is challenging to integrate the other sensing devices like air tactile sensor, infrared sensor, or even a camera [12]–[18]. In addition, clear environments are required in these devices in order to provide good results from estimation algorithms. In this paper, these requirements are avoided. The proposed sensing device has been successfully validated on real-time experiments and suction tasks are completely carried out. It is noted that the possibility of sensing tip misses or slips off the carina rarely happens during real-time experiments because the catheter tip first touches the carina before it possibly slides into bronchus. In addition, the sensing device is very sensitive and able to sense a small force of 0.08017 N. Once the sensing device is activated, the motor A is immediately stopped.

The validation results demonstrated that the proposed system and control approaches meet technical/clinical requirements given in Section II-A. The system is able to stop the catheter tip at desired positions and successfully carried out suction tasks using the recommended pressure, duration, and speed. For example, the catheter tip using compensation control is able to travel a length of 9 cm and this length stays within the specification from real clinical (5–10 cm). Although the designed mechatronic tracheostomy system is able to automatically carry out the suction tasks and promises potential benefits to the mechanical ventilation areas, some problems must be carefully considered when it is applied to real clinical applications. To apply the compensation control scheme, offline identification is needed for the model parameters. Currently, the identification process takes around 3 min. To reduce the identified time, an advanced algorithm should be developed for faster convergences. For the use of the sensing device, an advanced algorithm should be included to stop the catheter if the electric circuit is not closed. Other problems associated with the clinical application are the cleaning processes for the catheter. The catheter should be easily removed for cleaning and easy replacements

and should be isolated from the atmosphere to prevent the invasion and spread of contaminants. An automated process would mean a consistent delivery of suctioning, which would prove beneficial to the patient when it complements manual suctioning. At the end of the procedure, the device can be dismantled for easy cleaning. The secretions suctioned can be collected for further analysis. These issues must be carefully considered in the clinical applications. It is noted that the use of first or second approach will depend on specific cases. If the travel length is known in advance, the first approach should be used because it is cheaper compared to the case of using sensing device (higher cost on fabrication, testing, sterilization, and integration).

For the future works, we aim to test the prototype on animal models and then on the human. These clinical works will be carried out at National University Hospital, Singapore. In addition, our future goal is to use fiber optic or flexible soft conductive sensor to provide the displacement/force information for the operation. Nonlinear and adaptive control algorithms will be also applied to enhance the tracking performances of the system.

ACKNOWLEDGMENT

The authors would like to thank medical doctors S. W. Ting and J. Phua from National University Hospital, Singapore, for their suggestions and discussions during the research.

REFERENCES

- [1] P. De Leyn *et al.*, “Tracheotomy: Clinical review and guidelines,” *Eur. J. Cardio-Thoracic Surg.*, vol. 32, no. 3, pp. 412–421, 2007.
- [2] N. Adhikari *et al.*, “Critical care and the global burden of critical illness in adults,” *Lancet*, vol. 376, no. 9749, pp. 1339–1346, 2010.
- [3] J. Stauffer *et al.*, “Survival following mechanical ventilation for acute respiratory failure in adult men,” *Chest*, vol. 104, no. 4, pp. 1222–1229, 1993.
- [4] A. Plummer and D. Gracey, “Consensus conference on artificial airways in patients receiving mechanical ventilation,” *Chest*, vol. 96, no. 1, pp. 178–180, 1989.
- [5] P. Terragni *et al.*, “Early vs late tracheotomy for prevention of pneumonia in mechanically ventilated adult ICU patients: A randomized controlled trial,” *J. Amer. Med. Assoc.*, vol. 303, no. 15, pp. 1483–1489, 2010.
- [6] F. Blot and C. Melot, “Indications, timing, and techniques of tracheostomy in 152 french ICUs,” *Chest*, vol. 127, no. 4, pp. 1347–1352, 2005.
- [7] L. Fischler *et al.*, “Prevalence of tracheostomy in ICU patients. A nationwide survey in Switzerland,” *Intensive Care Med.*, vol. 26, no. 10, pp. 1428–1433, 2000.
- [8] A. Delaney *et al.*, “Percutaneous dilatational tracheostomy versus surgical tracheostomy in critically ill patients: A systematic review and meta-analysis,” *Critical Care*, vol. 10, no. 2, pp. 1–13, 2006.
- [9] C. Russell, “Providing the nurse with a guide to tracheostomy care and management,” *Brit. J. Nursing*, vol. 14, no. 8, pp. 428–433, 2005.
- [10] T. Day *et al.*, “Tracheal suctioning: An exploration of nurses’ knowledge and competence in acute and high dependency ward areas,” *J. Adv. Nursing*, vol. 39, no. 1, pp. 35–45, 2002.
- [11] C. Clec’h *et al.*, “Tracheostomy does not improve the outcome of patients requiring prolonged mechanical ventilation: A propensity analysis,” *Critical Care Med.*, vol. 35, no. 1, pp. 132–138, 2007.
- [12] M. Shamir *et al.*, “Automatic computerized endotracheal tube position verification: An animal model evaluation,” *Anesthesia Analgesia*, vol. 113, no. 6, pp. 1411–1415, 2011.
- [13] D. Lederman *et al.*, “Automatic endotracheal tube position confirmation system based on image classification—A preliminary assessment,” *Med. Eng. Phys.*, vol. 33, no. 8, pp. 1017–1026, 2011.
- [14] D. Lederman, “Endotracheal intubation confirmation based on video image classification using a parallel GMMs framework: A preliminary evaluation,” *Ann. Biomed. Eng.*, vol. 39, no. 1, pp. 508–516, 2011.

- [15] Y. Song *et al.*, "A novel method to position an endotracheal tube at the correct depth using an infrared sensor stylet," *Can. J. Anesthesia*, vol. 60, no. 5, pp. 444–449, 2013.
- [16] H. Kato *et al.*, "A visual stethoscope to detect the position of the tracheal tube," *Anesthesia Analgesia*, vol. 109, no. 6, pp. 1836–1842, 2009.
- [17] P. Goethals *et al.*, "A novel airway device with tactile sensing capabilities for verifying correct endotracheal tube placement," *J. Clin. Monit. Comput.*, vol. 28, no. 2, pp. 179–185, 2014.
- [18] J. Moll *et al.*, "Assessment of three placement techniques for individualized positioning of the tip of the tracheal tube in children under the age of 4 years," *Pediatric Anesthesia*, vol. 25, no. 4, 2015.
- [19] T. N. Do *et al.*, "An investigation of friction-based tendon sheath model appropriate for control purposes," *Mech. Syst. Signal Process.*, vol. 42, no. 1–2, pp. 97–114, 2014.
- [20] S. Kesner and R. Howe, "Position control of motion compensation cardiac catheters," *IEEE Trans. Robot.*, vol. 27, no. 6, pp. 1045–1055, Dec. 2011.
- [21] T. N. Do *et al.*, "A novel approach of friction model for tendon-sheath actuated surgical systems: Modeling and parameter identification," *Mechanism Mach. Theory*, vol. 85, pp. 14–24, 2015.
- [22] T. N. Do *et al.*, "Dynamic friction-based force feedback for tendon-sheath mechanism in notes system," *Int. J. Comput. Elect. Eng.*, vol. 6, no. 3, pp. 252–258, 2014.
- [23] B. Bardou *et al.*, "Improvements in the control of a flexible endoscopic system," in *Proc. IEEE Int. Conf. Robot. Autom.*, Saint Paul, MN, USA, May 2012, pp. 3725–3732.
- [24] T. N. Do *et al.*, "Adaptive control for enhancing tracking performances of flexible tendonsheath mechanism in natural orifice transluminal endoscopic surgery (notes)," *Mechatronics*, vol. 28, pp. 67–78, 2015.
- [25] T. L. Nguyen *et al.*, "Modelling, design, and control of a robotic running foot for footwear testing with flexible actuator," in *Proc. 1st Int. Conf. Sports Sci. Technol.*, Singapore, 2014, pp. 505–514.
- [26] T. N. Do *et al.*, "Design and control of a novel mechatronic tracheostomy tube-inserted suction catheter for automated tracheal suctioning," in *Proc. IEEE 7th Int. Conf. Cybern. Intell. Syst.-7th IEEE Int. Conf. Robot., Autom. Mechatronics*, Angkor Wat, Cambodia, 2015, pp. 228–233.
- [27] V. Hassani *et al.*, "A survey on hysteresis modeling, identification and control," *Mech. Syst. Signal Process.*, vol. 49, no. 1, pp. 209–233, 2014.
- [28] M. Rakotondrabe, "Bouc-wen modeling and inverse multiplicative structure to compensate hysteresis nonlinearity in piezoelectric actuators," *IEEE Trans. Autom. Sci. Eng.*, vol. 8, no. 2, pp. 428–431, 2011.
- [29] T. N. Do *et al.*, "Adaptive control of position compensation for cable-conduit mechanisms used in flexible surgical robots," in *Proc. 11th Int. Conf. Informat. Control, Autom. Robot.*, Vienna, Austria, 2014, pp. 110–117.
- [30] T. Tjahjowidodo *et al.*, "Quantifying chaotic responses of mechanical systems with backlash component," *Mech. Syst. Signal Process.*, vol. 21, no. 2, pp. 973–993, 2007.
- [31] T. N. Do *et al.*, "Enhanced performances for cable-driven flexible robotic systems with asymmetric backlash profile," in *Proc. IEEE Int. Conf. Technol. Practical Robot Appl.*, Woburn, MA, USA, May 2015, pp. 1–6.
- [32] T. Vo Minh *et al.*, "Control of a pneumatic artificial muscle (PAM) with model-based hysteresis compensation," in *Proc. IEEE/ASME Int. Conf. Adv. Intell. Mechatronics*, Jul. 2009, pp. 1082–1087.
- [33] K. Johansson and C. Canudas-de Wit, "Revisiting the LuGre friction model," *IEEE Control Syst. Mag.*, vol. 28, pp. 101–114, Dec. 2008.
- [34] T. N. Do *et al.*, "Hysteresis modeling and position control of tendon-sheath mechanism in flexible endoscopic systems," *Mechatronics*, vol. 24, no. 1, pp. 12–22, 2014.
- [35] M. Rakotondrabe *et al.*, "Simultaneous displacement/force self-sensing in piezoelectric actuators and applications to robust control," *IEEE/ASME Trans. Mechatronics*, vol. 20, no. 2, pp. 519–531, Apr. 2015.
- [36] T. N. Do *et al.*, "Position control of asymmetric nonlinearities for a cable-conduit mechanism," *IEEE Trans. Autom. Sci. Eng.*, Jun. 2015, doi:10.1109/TASE.2015.2438319.
- [37] T. N. Do *et al.*, "Real-time enhancement of tracking performances for cable-conduit mechanisms-driven flexible robots," *Robot. Comput. Integr. Manuf.*, vol. 35, pp. 197–207, Feb. 2016.
- [38] D. R. Hess and N. P. Altobelli, "Tracheostomy tubes," *Respiratory Care*, vol. 59, no. 6, pp. 956–973, 2014.
- [39] C. M. Pedersen *et al.*, "Endotracheal suctioning of the adult intubated patient—What is the evidence?" *Intensive Critical Care Nursing*, vol. 25, no. 1, pp. 21–30, 2009.
- [40] S. G. C. Palazzo and B. Soni, "Pressure changes during tracheal suctioning a laboratory study," *Anaesthesia*, vol. 68, no. 6, pp. 576–584, 2013.
- [41] John hopkins medicine (2015), suctioning. [Online]. Available: <http://www.hopkinsmedicine.org/tracheostomy/living/suctioning.html>
- [42] G. Tao and P. Kokotovic, "Adaptive control of systems with backlash," *Automatica*, vol. 29, no. 2, pp. 323–335, 1993.
- [43] G. Tao and P. Kokotovic, "Adaptive control of system with unknown output backlash," *IEEE Trans. Automat. Contr.*, vol. 40, no. 2, pp. 326–330, Feb. 1995.
- [44] F. Ikhouane *et al.*, "Variation of the hysteresis loop with the Bouc–Wen model parameters," *Nonlinear Dyn.*, vol. 48, no. 4, pp. 361–380, 2007.
- [45] T. N. Do *et al.*, "Nonlinear friction modelling and compensation control of hysteresis phenomena for a pair of tendon-sheath actuated surgical robots," *Mech. Syst. Signal Process.*, vol. 60–61, no. 2015, pp. 770–784, 2015.
- [46] V. Hassani and T. Tjahjowidodo, "Structural response investigation of a triangular-based piezoelectric drive mechanism to hysteresis effect of the piezoelectric actuator," *Mech. Syst. Signal Process.*, vol. 36, no. 1, pp. 210–223, 2013.
- [47] T. N. Do *et al.*, "Nonlinear modeling and parameter identification of dynamic friction model in tendon sheath for flexible endoscopic systems," in *Proc. 10th Int. Conf. Informat. Control, Autom. Robot.*, Reykjavik, Iceland, 2013, pp. 5–10.
- [48] T. N. Do *et al.*, "Dynamic friction model for tendon-sheath actuated surgical robots: Modelling and stability analysis," in *Proc. 3rd Int. Symp. Robot. Mechatronics*, Singapore, 2013, pp. 302–311.
- [49] E. Breatnach *et al.*, "Dimensions of the normal human trachea," *Amer. J. Roentgenol.*, vol. 142, no. 5, pp. 903–906, 1984.



Thanh Nho Do (M'15) received the Ph.D. degree from Nanyang Technological University (NTU), Singapore, in 2015.

He is currently a Postdoctoral Research Fellow at the School of Mechanical & Aerospace Engineering, NTU. His research interests include the development of magnetic actuators for capsule endoscope, drug delivery system, flexible soft sensors, nonlinear hysteresis, and adaptive control in surgical devices and flexible robotic systems.



Tian En Timothy Seah received the M.Eng. degree in mechanical engineering and M.Res. degree in medical robotics and image guided intervention from Imperial College London, London, U.K., in 2013 and 2014, respectively.

He is currently a Research Associate at Nanyang Technological University, Singapore. His research interests include the design and development of novel medical devices, flexible surgical robotic systems, and high compliance force sensors.



Soo Jay Phee (M'02) received the Ph.D. degree from the Scuola Su-periore Sant'Anna, Pisa, Italy, under a European Union scholarship.

He is currently a Full Professor and a Chair of the School of Mechanical & Aerospace Engineering, Nanyang Technological University, Singapore. He is the Principal Investigator of some projects and CEO & Cofounder of EndoMaster Pte, Ltd. His research interests include medical robotics and mechatronics in medicine.